



PERFORMANCE ANALYSIS OF FIBER OPTIC CURRENT SENSOR USING SAGNAC INTERFEROMETER

S. K. Idris@Othman*¹, H. Haroon¹, H. Abdul Razak¹, A. S. Mohd Zain¹, H. Jaafar²

¹Fakulti Kejuruteraan Elektronik dan Kejuruteraan Komputer, Universiti Teknikal Malaysia Melaka, Hang Tuah Jaya, 76100 Durian Tunggal, Melaka, Malaysia.

²Fakulti Kejuruteraan, Universiti Putra Malaysia, 43400 UPM Serdang, Selangor, Malaysia.

*sitikhadjah@utm.edu.my

Article history:

Received Date:

2021-10-07

Accepted Date:

2022-01-01

Keywords:

Electromagnetic

Interference

(EMI), Fiber

Optic Current

Sensor (FOCS),

Polarization,

OptiSystem,

Sagnac

Abstract— In conventional current sensors, the accuracy, sensitivity, reliability, and safety are greatly affected by electromagnetic interference phenomena. The advancement of fiber optic technology in recent years opened up a better solution to this problem. The motivation of this project is to implement and enhance fiber optic as a current sensor. A fiber optic interferometer is applied to receive inputs from a modulator, which resemble the presence of an electromagnetic field around a conductor carrying an electrical current. This research is to design and demonstrate a fiber optic current sensor using Sagnac

Interferometer	interferometric scheme. The design is simulated using Optisystem software. The performance of the fiber optic current sensor was observed and analyzed. Analysis has focused on the output waveform, transmission losses, power consumption, and sensitivity of the device based on the Pulse mode and CW mode. CW mode laser had a more stable and steady waveform however the power consumption and transmission losses are higher compared to pulse mode. For pulse mode, at a higher frequency, the sensitivity of the proposed fiber-optic current sensor design is decreased.
----------------	---

I. Introduction

A transducer is defined as a device that receives energy from physical phenomena and transmits it in the form of another type of energy to a system. Two important elements for a transducer are the sensing element and the transduction element [1]. An electrical transducer is described as a device that converts any physical, mechanical, or optical quantities into a proportional electrical quantity such as voltage or current [2]. Current sensors apply the electrical

phenomena to sense and transform the current into an output voltage, which is easily measured while maintaining the linearity condition. Sensing an electrical quantity can be divided into direct and indirect methods [3, 4].

An electrical transducer is widely used and is long being applied in various engineering fields. However, it has some bad implications and disadvantages, notably for the incapacity of measurement for extreme physical conditions. The instrument circuit requires some

additional components and techniques [5-8]. Consequently, the installation and maintenance of the devices becoming more complicated and costly. The presence of Electromagnetic Interference (EMI) brings another problem, as the components inside a current sensor device are becoming an unintentional antenna and capturing EMI radiation from external surroundings [9]. Furthermore, sensitivity, security, and reliability aspects are also compromised due to numerous potential of external perturbation hence, degrading the performance of the sensor.

The idea of manipulating light wave properties made optical sensing is possible, by means of determining the relationship between the variable measured with changes in lightwave [10]. The basic structure for fiber optic sensors is shown in Figure 1. A light source is injected into an optical fiber and the light wave travels to the transducer, which manipulates the light characteristic related to external perturbation from phenomena being measured. The changing

light is detected by a detector, converted into an electrical signal, and then processed by an electronic processing unit to extract the information contained [10]. Many properties of light can be exploited, such as intensity, phase, wavelength, frequency, polarization, and even bandwidth [9].

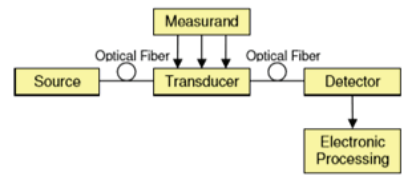


Figure 1: Basic principle of the optical transducer

Fiber optic sensors can be classified into intrinsic and extrinsic and have numerous advantages, which are smaller size, lightweight, secure, and reliable over metallic core cable [11-12], and has relatively low cost and low power consumption. In terms of transmission, fiber optic provides wider bandwidth, hence, suitable for long-distance connection due to low transmission and absorption loss [14]. The immunity against EMI is the most highlight advantage [10]. Passive element used in

fiber optic construction is good for electrical isolation and prevents capturing electromagnetic radiation. Ruggedness to vibration and shock gave it the ability to operate in a dangerous environment [10]. The absence of saturation effect allows fiber optic sensors to measure alternate current (AC) or direct current (DC), hence making it suitable for high voltage applications.

Faraday Effect is the impact of the refractive index differences that occurred when the optical light is circularly polarized into the right and left side with the presence of a magnetic field inside the magneto-optic material [15-17]. As the light travel and undergoes rotation with angle (θ), the light traveled back in opposite direction will have ($-\theta$), described as non-reciprocal behavior.

The linear polarized rotation angle of the light wave is proportional to the magnetic field strength and cosine angle of propagation for the light wave and the field.

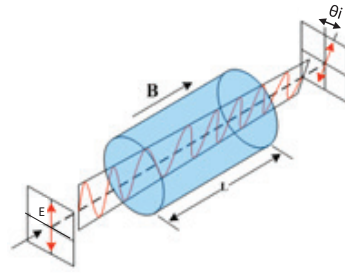


Figure 2: Polarization changes of lightwave

$$\theta_f = \int_L^1 \vec{V} \vec{B} \cdot d\vec{l} \quad (1)$$

where; V is the Verdet constant, B is the magnetic field and $d\vec{l}$ is the differential vector of propagation. The V measures the strength of the Faraday Effect in materials, and depends on the refractive index dispersion, given by [15]:

$$V = - \frac{e\lambda}{2mc} \frac{dn}{d\lambda} \quad (2)$$

where; e is the electronic charge, m is the mass of the electron and c is the velocity of the light. The effect of Faraday's law towards the azimuth of the optical light was interrogated through a polarimetric detection technique or interferometric detection technique. The interferometer detection scheme has become a popular choice to achieve a high degree of sensitivity, reliability,

and high performance, either for a linear or non-linear variable of environmental phenomena [11], [16].

In general, four types of structure were used to sense electrical variables, which are the All-Fiber, Bulk Optic, Magnetic Force, and Hybrid. The Fiber-optic current sensor (FOCS) has the advantages of high accuracy, high bandwidth, fast fault response time, large dynamic range, wide frequency response range, and no magnetic saturation and resonance phenomenon, and many more, thus making it a significant sensing technique for current detection and measurement. An advanced FOCS is based on the recirculating architecture of the fiber loop for significantly enhancing the current sensitivity. Depending on the application, FOCS using Sagnac Interferometer is modified for better performance. Among the architecture are FOCS using Sagnac interferometer with and without fiber polarization rotator (FPR) and FOCS with differentiating Sagnac interferometer. FOCS based on

Faraday magneto-optical effect has plenty of advantages however the residual linear birefringence and environmental vibration-sensitive are the drawbacks. This research is to design and demonstrate a FOCS with a passive fiber optic Sagnac interferometer scheme. The design is simulated using Optisystem software. The performance of the fiber optic current sensor was observed and analyzed in terms of the output waveform, transmission losses, power consumption, and sensitivity of the device based on the Pulse mode and CW mode.

II. SAGNAC Interferometer Detection Scheme

Sagnac Effect can be explained by considering a perfectly circular path of the fiber as in Figure 3. The phase of the light wave is linearly dependent on the rotation of the path as it propagates slowly in rotation. Phase differences are produced when the two counter-propagating waves exist in the same circular path. The two-propagating waves can be either

clockwise or counter-clockwise propagation [11]. As both of the modes are propagating within the radius of the circular (R) and a rate of angular velocity (Ω), the duration of the wave required to traverse a path differs for both modes, either one mode being longer than the other one. Based on this condition, the phase difference ($\Delta\phi$) occurred and can be determined by using an interferometer.

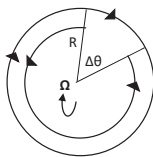


Figure 3: Pathway of the two counter-propagating waves

Sagnac Interferometer is arranged by connecting a certain length of fiber to the two output ports of the coupler, intentionally to form a loop as in Figure 4. Sagnac Interferometer manipulates the phenomena of self-phase modulation and cross-phase modulation, often in non-linear [11].

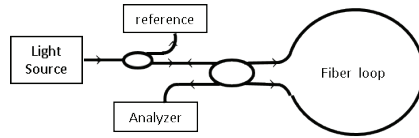


Figure 4: Passive fiber-optic Sagnac interferometer

There is two notable behavior of the Sagnac Interferometer scheme compared to other schemes [11]. Firstly, all light wave exits the resonator in a single round trip. Secondly, two counter-propagating parts have the same optical route and coherently interfere at the coupler. The reflection and transmission of the input beam are determined by measuring the relative phase difference between the counter-propagating parts. The phase difference of the counter-propagating parts is given by [14]:

$$\Delta\phi = \frac{2\pi N A \Omega}{\lambda C} \quad (3)$$

where; N is the number of turns in the fiber loop, A is the area covered by the coil, Ω is the angular velocity, λ is the wavelength in free space and C is the velocity of the light. The main reason for the two counter-propagating parts are needed is

that one is for the affection of external variables such as temperature, strain, and current, while the other one is saved as reference [11]. Most of the Sagnac Interferometer applied a 3dB coupler, as the input is reflected. The sensitivity of the Sagnac Interferometer is defined as the ratio of phase difference ($\Delta\theta$) to the angular velocity (Ω). Increment numbers of turns (N), length of the fiber, and the laser frequency contribute to a good sensitivity.

Sagnac interferometer has several advantages over other interferometric schemes. The fiber itself is usually used as a sensing element with one coupler, hence giving the simplest structure and ease to be fabricated compared to other types of the interferometer. Moreover, it also provides

environmental robustness as the fiber itself is immune to environmental changes. The most distinctive advantage of the Sagnac interferometer is its capability to sense a few variables simultaneously. A Sagnac scheme is merged with a Mach-Zehnder interferometer to create a hybrid type interferometer designed to sense strain and temperature simultaneously. Simultaneous measurement capability also allows the Sagnac interferometer to be designed for a wide range of measurements and applications [10].

III. Sensor Structure Design

A conductor carrying an electrical current is placed in the middle of the loop as shown in Figure 5.

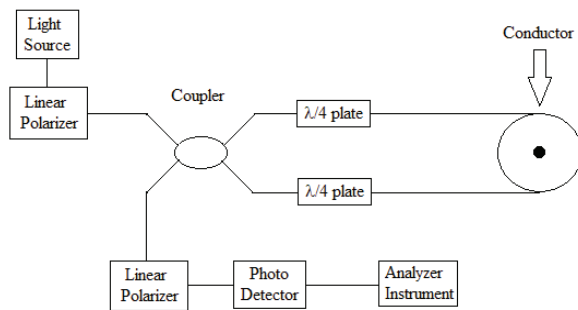


Figure 5: Theoretical structure design

The flow of the current in a conductor, with a certain length, will create a phenomenal of Faraday Effects. In terms of the significance of the Faraday Effect in this model, it will influence a phase shift to the waves which is a non-reciprocal change. As both waves are shifted in phase, each of them will experience either positive changes or negative changes.

These changes are being corresponding to the strength of the magnetic field related to the Faraday Effect. However, for practical usage, the theoretical structure can be modified to satisfy the limitation. The limitation that is discussed here is the absence of the Sagnac structure module in Optisystem software.

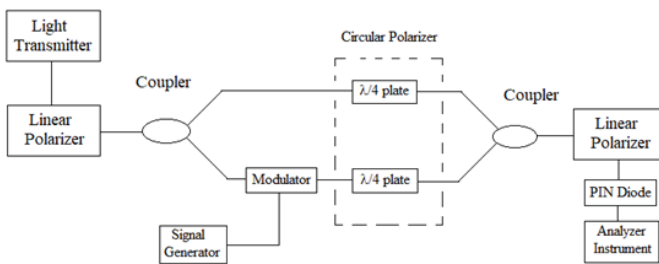


Figure 6: Practical structure design for simulation

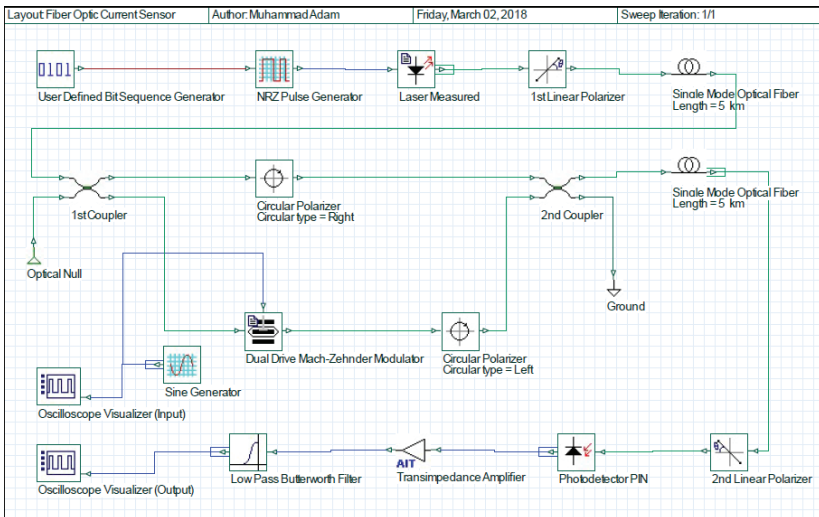


Figure 7: Simulation layout for Sagnac Interferometer fiber-optic current sensor

Figure 6 shows the practical structure design for simulation. The flow of the circuit started with a light source is injected into fiber optic and passes through a polarizer, which polarizes the light wave linearly. The linear lightwave then is divided into two waves equally in intensity with the help of a coupler. Modifications are necessary to be implemented to ease the simulation stage later on. A modulator with a signal generator is used to replace a conductor carrying current, by introducing an external waveform into the sensing path. Hence, two different optical paths are possible to be created. Next, both light waves are polarized circularly by $\lambda/4$ plate and recombined back by a coupler.

The resulting light wave is linearly polarized once again. Finally, a photo-detector is used to measure the intensity of output light and convert it into a small amount of electrical current. The current generated then will enter an analyzer instrument, where it will undergo an amplification and

filtration process before finally being presented as a waveform in an oscilloscope. The simulation layout using Optisystem Software is shown in Figure 7.

The simulation layout started with a light source of LASER which is equipped with a User Defined Bit Sequence Generator and NRZ Pulse Generator. Input in the form of a binary sequence is converted into an electrical signal first before being transformed into an optical wave signal. This configuration is named Pulse mode. Meanwhile, for Continuous-Wave (CW) mode, the light source is replaced by CW LASER component.

The light wave is polarized in linear form by the first Linear Polarizer and is injected into Single Mode Fiber (SMF) optic with a certain length for transmission purposes. The linearly polarized light wave is divided into two beams that have the same intensity and frequency by the first coupler. One of the pathways for the light wave consists of a right-handed circular polarizer. Whereas on

the other path, the lightwave is connected into Mach-Zehnder Modulator first before entering a left-handed circular polarizer. Sine Generator is used to provide a sinusoidal modulating signal to the modulator. Both pathways then are recombined back through the second coupler.

The resulting light wave from the loop travels back via a SMF optic and is linearly polarized back by a second Linear Polarizer. The photo-detector (PIN) detects the resulting modulated wave, removing the carrier and processing information signal into electric current. However, the current needed to be amplified first by Trans-Impedance Amplifier (TIA), which also converts the current into voltage. A Low-Pass Butterworth Filter then is used for filtering the signal by allowing or blocking frequencies. Finally, the output is observed and analyzed via an electrical Oscilloscope Visualizer. Both oscilloscope visualizers are used to make a comparison between the input sinusoidal signal and output waveform obtained.

The performance analysis for simulation of the current sensor structure can be divided into three parts. The first part consists of observation on measurement equipment. The observation is focused on the light source, state of polarization, input sine signal generator on Mach-Zehnder Modulator, photodiode conversion, and final output waveform. The second part consists of an analysis of losses and power utilization. The input power from the light source transmitted in SMF is measured, and the output power at the receiving end is recorded. The loss is calculated by using

$$Loss (dB) = 10 \log \frac{P_{out}}{P_{in}} \quad (4)$$

where; P_{in} is the input power while P_{out} is the output power measured. The third part, which is the sensitivity, depends on the frequency of the Sine Generator. Frequency plays an important role as it is related to wavelength parameters, which are correlated with the phase difference. The frequency of the sine generator is arranged and changed to analyze its impact on the final

output current. There is ten proposed input frequency chosen between 150MHz to 1 GHz. The relationship between frequency and phase difference exists for two optical waves in the Sagnac loop is given by

$$\Delta\phi = 360^\circ \times F \times \Delta t \quad (5)$$

where; $\Delta\phi$ is total phase changes, F is the frequency and Δt is the difference of time of input and output sine waves. The sensitivity ranges for the design are determined and concluded.

IV. Result and Discussion

A. Output Waveform Comparison

The primary difference between Pulse mode laser and CW mode laser is their pumping mechanism. CW mode laser continuously supplies laser beam whereas, for Pulse mode, light intensity is concentrated for a short duration of time. Therefore, when the output light wave that was detected after passing through an interferometric scheme is analyzed, the spectrum and waveform differ for both modes. The output waveforms after

lightwave conversion are compared between Pulse mode (as seen in Figure 8) and CW mode (as seen in Figure 9).

Based on a comparison of the figures, CW mode laser had a more stable and steady waveform compared to Pulse mode. It can be considered that the light wave transmitted in pulse mode might support the phase shift process that occurred in Sagnac interferometric scheme but is insufficient to maintain stability. Thus, it can be concluded that this application depends on a beam whose output power is constant over time, which made CW mode laser a better option.

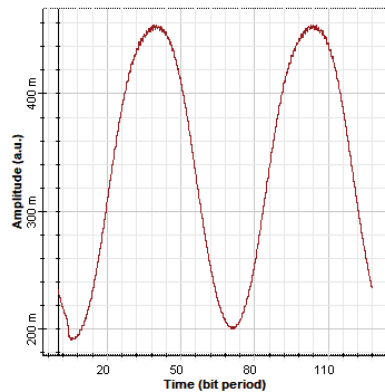


Figure 8: Output waveform using Pulse mode source

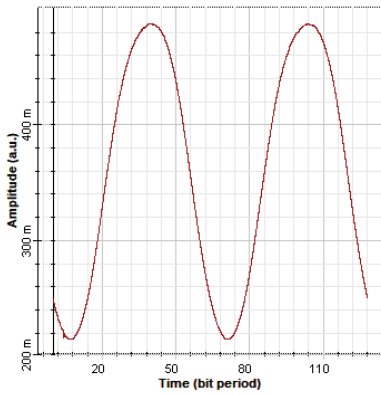


Figure 9: Output waveform using CW mode source

B. Losses and Power Consumption

This design is applied only for optical transmission and neglects power consumption other than non-fiber components

that were involved. The losses in this section are calculated by using Equation 4. The input power, output power, and losses for both modes are presented in Table 1.

In correlation with the previous discussion, laser operated in CW mode consumes higher power because of pumping mechanism continuously supplies a constant light beam over time. Therefore, CW mode laser has higher power consumption and higher transmission losses compared to pulse mode.

Table 1: Losses calculated for both modes

Parameters	Pulse Mode	Continuous-Wave
Input Power (mW)	5.48	10.00
Output power (μ W)	563.14	601.81
Losses (dB)	-9.88	-12.2

C. Sensitivity

The sensitivity considered is from fiber-optic current sensor design with laser on Pulse mode operation due to lower losses rate than CW mode. Table 2 shows the frequency of the sine generator compared to the output waveform and the resulting phase differences.

The slope resulting from deriving the relationship between frequency and phase difference is the sensitivity of the sensor presented in Figure 10. As phase differences decrease, at a higher frequency, the sensitivity of the proposed fiber-optic current sensor design is decreased.

Table 2: Frequency ranges and phase differences

f	Δt	$\Delta\theta$
150 MHz	2.4453E-9	132.046
250 MHz	1.4172E-9	127.55
350 MHz	9.2179E-10	116.15
450 MHz	4.8604E-10	78.74
550 MHz	3.3519E-10	66.37
650 MHz	2.6815E-10	62.75
750 MHz	1.6447E-10	44.41
850 MHz	1.1513E-10	35.23
950 MHz	9.8679E-11	33.75
1 GHz	6.5786E-11	23.68

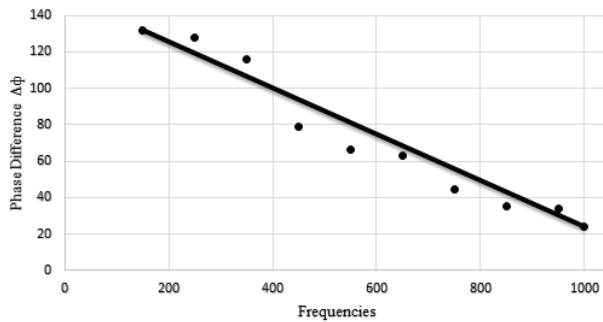


Figure 10: Sensitivity (slope)

V. Conclusion

Performance analysis of the Sagnac interferometer can be viewed diversely. In terms of stability, the Sagnac interferometer with CW mode laser as a light source provided the best result. However, configuration with pulse mode laser gave another advantage over CW mode, which are low transmission loss, low power consumption, and better

sensitivity. Furthermore, the deficit suffered by the design with pulse mode can still be improved by applying digital signal recovery technique. Therefore, pulse mode laser is a better selection to achieve the best performance for the Sagnac interferometer current sensor compared to CW mode.

VI. References

[1] M. Ginter, Fiber Optic Sensor for Measuring Currents with mains

- Frequencies, in Proc. SPIE Photonics Applications in Astronomy, Communications, Industry, and High-Energy Physics Experiments, 2018 Vol.10808.
- [2] J. Nedoma, M. Fajkus, R. Martinek, Measurement of Electric Current using Optical Fiber: A Review, in PRZEGLĄD ELEKTROTECHNICZNY, Vol. 93, Issue (11) 2017, pp. 140-145.
- [3] L. Wang, M. Cao, Q. Liu, G. Wei, B. Li, C. Lin, Modeling and Experimental Verification of Polarization errors in SAGNAC Fiber Optic Current Sensor, in *Optik*, Vol.126, Issue (20), 2015, pp. 73-79.
- [4] M. Biglarbegan, S. Nibir, H. Jafarian & B. Parkhideh, Layout Study of contactless magneto-resistor current sensor for high frequency converters. Conference Paper: ECCE. Sept. 2016.
- [5] M. Bichurin, R. Petrov, V. Leontiev, & O. Sokolov, Magnetolectric Current Sensors. in MDPI: *Sensors* **17**(6). 2017.
- [6] L. Dalessandro, N. Karrer, & J. W. Kolar, High-performance planar isolated current sensor for power electronic application. *IEEE Transaction on Power Electronic*, **22**(5), 1682, 2007.
- [7] K. Li, Y. Dai, Y. Wang & S. Huang, Analysis and Modelling of leakage current sensor under pulsating direct current. *AIP Advances* **7**, 056649, 2017.
- [8] R. M. Silva, H. Martins, I. Nascimento, J. M. Baptista, A. L. Ribeiro, J. L. Santos, P. Jorge, O. Frazao, Optical Current Sensors for High Power System: A Review, in *App. Sci.*, Vol. 2, 2012, pp. 602-628.
- [9] T. Chang, H. L. Cui, J. Chen, Phase Compensation Scheme for Fiber Optic Interferometric Vibration Demodulation. *IEEE Sensors Journal* 2017 pp.1.
- [10] J. Xia, Q. Wang, X. Liu, H. Luo, Fiber Optic Fabry-Perot Current Sensor Integrated with Magnetic Fluid using a Fiber Bragg Grating Demodulation. in *Sensors*, **15**, 2015, pp. 16632-16641.
- [11] S. Tofghi, A. R. Bahrampour, & F. Shojaee, Optimum quantum state of light for gravitational-wave interferometry. in *Optics Communications*, Vol. 283, No. 6, 2010, pp. 1012-1016.
- [12] Y. Yang, L. Lu, F. Yang, Y. Chen, The fiber optic Sagnac interferometer and its sensing application. *Optoelectronics Global Conference (OGC)*. 2015.
- [13] P. Perez-Millan, L. Martinez-Leon, A. Diez, J. L. Cruz, M. V. Andres, A fiber-optic current sensor with frequency-codified output for high-voltage systems. in *IEEE Photon. Technol. Lett.* Vol.14, 2002, pp. 1339–1341.
- [14] F. Ferdous and A. H. Rose, Cable Fault Detection: Optical Fiber Current Sensor Cable Link Noise Reduction, 2020 *IEEE/PES Transmission and Distribution Conference and Exposition*

- (T&D), 2020, pp. 1-5,
- [15] A. Miliou, In-Fiber Interferometric-Based Sensors: Overview and Recent Advances. in *Photonics*. Vol.8, issue (7), 2021, pp. 265.
- [16] H. Xueming, W. Guochen, G. Wei, W. Yongguang, and G. Hongze, The effect analysis of impact on a fiber optic current sensor, in *Optik*, Volume 238, 2021, pp.166724
- [17] J. S. N'cho, I. Fofana, Review of Fiber Optic Diagnostic Techniques for Power Transformers, in *Energies*. Vol.13, issue (7), 2020, pp.1789.

